



## Phase-Separation Perspective on Dynamic Heterogeneities in Glass-Forming Liquids

C. Cammarota,<sup>1,2,\*</sup> A. Cavagna,<sup>2,3</sup> I. Giardina,<sup>2,3</sup> G. Gradenigo,<sup>4,5,†</sup> T. S. Grigera,<sup>6</sup> G. Parisi,<sup>1,2</sup> and P. Verrocchio<sup>4,5,7</sup>

<sup>1</sup>Dipartimento di Fisica, Università di Roma “Sapienza,” piazzale Aldo Moro 5, 00185, Roma, Italy

<sup>2</sup>Centre for Statistical Mechanics and Complexity (SMC), CNR-INFM, Roma, Italy

<sup>3</sup>Istituto Sistemi Complessi (ISC), CNR, Via dei Taurini 19, 00185 Roma, Italy

<sup>4</sup>Dipartimento di Fisica, Università di Trento, via Sommarive 14, 38050 Povo, Trento, Italy

<sup>5</sup>INFM CRS-SOFT, c/o Università di Roma “Sapienza,” 00185, Roma, Italy

<sup>6</sup>Instituto de Investigaciones Fisicoquímicas Teóricas y Aplicadas (INIFTA) and Departamento de Física,

Facultad de Ciencias Exactas, Universidad Nacional de La Plata, and CCT La Plata,

Consejo Nacional de Investigaciones Científicas y Técnicas, c.c. 16, suc. 4, 1900 La Plata, Argentina

<sup>7</sup>Instituto de Biocomputación y Física de Sistemas Complejos (BIFI), Zaragoza, Spain

(Received 21 January 2010; published 29 July 2010)

We study dynamic heterogeneities in a model glass former whose overlap with a reference configuration is constrained to a fixed value. We find that the system phase separates into regions of small and large overlap, indicating that a nonzero surface tension plays an important role in the formation of dynamical heterogeneities. We calculate an appropriate thermodynamic potential and find evidence of a Maxwell construction consistent with a spinodal decomposition of two phases. Our results suggest that even in standard, unconstrained systems dynamic heterogeneities are the expression of an ephemeral phase-separating regime ruled by a finite surface tension.

DOI: 10.1103/PhysRevLett.105.055703

PACS numbers: 64.70.pm, 61.20.Ja, 61.43.Fs, 64.60.My

The conspicuous lack of a growing correlation length, contrasting with the very steep increase of the relaxation time, has been a puzzle in the physics of structural glasses for quite a long time. Arguably, the first breakthrough has been the discovery of dynamic heterogeneities [1] and the detection of a growing dynamic correlation length  $\xi_d$  [2,3]. If we take two snapshots of the system separated by a time lag comparable to the  $\alpha$  relaxation time  $\tau_\alpha$ , the particle displacements vary enormously across the system, and the typical size  $\xi_d$  of the mobility-correlated regions increases on lowering the temperature.

More recently, by studying the thermodynamics of systems subject to amorphous boundary conditions [4,5], an entirely different, fully static, correlation length  $\xi_s$  has been discovered [6,7].  $\xi_s$  also grows upon cooling, even though its surge occurs at lower temperatures than  $\xi_d$ . The static correlation length has a natural interpretation as the size of the cooperatively rearranging regions [8], and within the random first-order theory [9] it is determined by the balance between a surface tension cost and a configurational entropy gain of a rearrangement.

Although the conceptual link between dynamics and thermodynamics is quite clear in mean-field systems [10] and some progresses have been made in more realistic systems [11], we are quite far from a unifying picture in real glass formers. In particular, it is important to understand whether or not there is any common factor behind the formation of dynamic and thermodynamic excitations. Here we answer positively to this question and show that the surface tension, which plays a key role in the thermodynamic rearrangements, is also crucial in the formation and growth of dynamic heterogeneities.

We start with the standard measurement of the dynamic correlation length  $\xi_d$ . Our glass former is the well-known soft-sphere model in 3D [12]. A useful tool to measure  $\xi_d$  is the overlap, which quantifies how much a configuration at time  $t$  is similar to the reference configuration at  $t = 0$ . If we partition the system in small cubic boxes and let  $n_i$  be the number of particles in box  $i$ , the local overlap is defined as  $q(\mathbf{r}_i, t) \equiv n_i(t)n_i(0)$ , where  $\mathbf{r}_i$  refers to the center of cell  $i$  [13]. The spatial map of the local overlap tells us how much different regions have decorrelated (with respect to the initial configuration) over a time  $t$ . In Fig. 1 (top), we

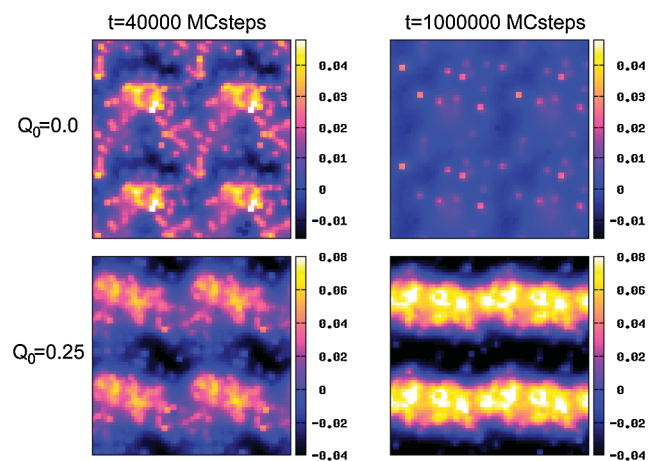


FIG. 1 (color). Fluctuations of the overlap field  $\delta q(\mathbf{r}, t) = q(\mathbf{r}, t) - \langle q(t) \rangle$  for a 2D slice of the system. Upper panels: Unconstrained system. Lower panels: Constrained system ( $\hat{Q} = 0.25$ ). Left panels:  $t = \tau_\alpha$ . Right panels: Large times.  $L = 16$ . Each panel displays four copies of the same system.

show two snapshots of the overlap field. At  $t = \tau_\alpha$  (left) there are large heterogeneous regions, which eventually fade away for longer times (right). To quantify their size, we compute the correlation function

$$G(\mathbf{r}, t) \equiv \langle q(0, t)q(\mathbf{r}, t) \rangle - \langle q(0, t) \rangle \langle q(\mathbf{r}, t) \rangle \quad (1)$$

or its Fourier transform  $S(k, t)$  (Fig. 2, left). In general, given a correlation function in Fourier space, it is well-established practice [14] to extract the correlation length  $\xi$  from the small- $k$  linear interpolation of  $S^{-1}$  vs  $k^2$ ,

$$S(k, t)^{-1} = A + Bk^2, \quad (2)$$

from which the correlation length is obtained as  $\xi(t)^2 = B/A$ . The validity of Eq. (2) is shown in the inset in Fig. 2, right [15]. The time-dependent correlation length  $\xi(t)$  represents the size of the dynamical heterogeneities at time  $t$ . This length scale grows as  $t$  approaches  $\tau_\alpha$  and the heterogeneities become more extended (inset in Fig. 2, left). The largest value of  $\xi(t)$  (reached at  $t \sim \tau_\alpha$ ) defines the dynamical correlation length  $\xi_d \equiv \xi(\tau_\alpha)$  [2,3,16].

For times  $t \gg \tau_\alpha$ , memory of the initial configuration fades away, so that the correlation function  $S(k, t)$  decays (Fig. 2, left). Although this makes it tricky to fix a reliable value of  $\xi(t)$  through Eq. (2), our results indicate that  $\xi(t)$  decreases beyond  $\tau_\alpha$  (Fig. 2, left inset). In any case, measuring  $\xi(t)$  for large  $t$  is *not* our concern here (see [16] vs [17] for this issue). Instead, the point we want to stress is that the *correlation* decreases for  $t \gg \tau_\alpha$ , irrespective of its spatial range  $\xi(t)$ : Heterogeneities blur as  $q(\mathbf{r}, t)$  becomes zero everywhere (Fig. 1, top right).

Let us now constrain the dynamics, so that the system cannot entirely lose memory of its initial configuration. This we do by imposing a lower bound on the global overlap:  $Q(t) = 1/V \int d\mathbf{r} q(\mathbf{r}, t)$ . In the unconstrained case  $Q(t)$  goes asymptotically to zero [18]. On the other hand, with the constraint  $Q(t) \geq \hat{Q}$  things change [19].

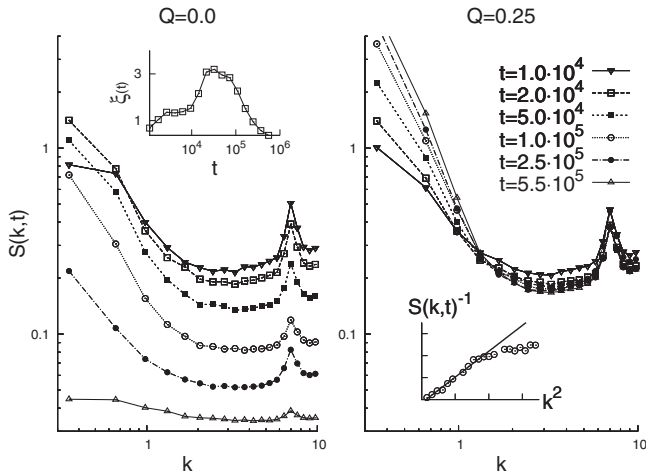


FIG. 2.  $S(k, t)$  at different times for the unconstrained (left) and constrained (right,  $\hat{Q} = 0.25$ ) cases. Left inset: Correlation length  $\xi(t)$  as extracted from Eq. (2). Right inset:  $S(k, t)^{-1}$  vs  $k^2$ .  $T = T_{MC}$  and  $L = 16$ .

Initially, the system does not feel the constraint: The overlap decays and everything proceeds as above, including the growth of the heterogeneities. However, at later times  $Q(t)$  hits its lower bound  $\hat{Q}$  and it cannot decrease further. What happens to the dynamical heterogeneities then?

There are two possibilities. One is that the correlation  $S(k, t)$  and its spatial range  $\xi(t)$  decay to zero as in the free case. Because of the constraint, however,  $q(\mathbf{r}, t)$  cannot become zero everywhere, so that heterogeneities must become very small, forming a salt-and-pepper configuration of the field  $q(\mathbf{r}, t)$  that ensures that its integral stays equal to  $\hat{Q}$ . The second possibility is that there is a *surface tension* between high- and low-overlap regions, favoring the merging of different heterogeneities. The system will then evolve towards a phase-separated, highly correlated state [20]; the correlation *will not* decay, and the dynamic correlation length  $\xi(t)$  will grow beyond  $\xi_d$ , up to an asymptotic value of the order of the system size.

The overlap field in the constrained case (Fig. 1, bottom right) shows that for large  $t$  the system phase separates into high- and low-overlap regions, forming stable dynamical heterogeneities of the order of the system size, as in a surface tension ruled scenario. Accordingly, the constrained correlation function does not go to zero for large times, but it saturates to a finite value (Fig. 2, right). Hence, even in the late time regime dynamic heterogeneities remain strongly correlated.

The correlation length in the constrained case confirms this scenario [21]. As long as  $\xi$  is much smaller than the system's size  $L$ , the large- $r$  form of the correlation function  $G(\mathbf{r}, t)$  is exponential, and thus the Lorenzian small- $k$  fit of (2) is consistent. In this case the quantity  $A/B$  is a good estimator of  $\xi^{-2}$ , with a systematic error of order  $L^{-2} \ll \xi^{-2}$ . However, as  $A/B = \xi^{-2}$  approaches  $L^{-2}$ , self-consistency breaks down: When  $\xi \sim L$ , the correlation function is no longer exponential for large  $r$  (the system is finite and periodic), so that the Lorenzian fit (2) is not consistent. For even larger  $\xi$ ,  $A/B$  is no longer a good estimator of  $\xi^{-2}$ . The important point is that the breakdown of the estimator signals that the correlation length has become comparable to the system's size.

We therefore need to compare  $A/B$  to  $L^{-2}$ . Figure 3 (left) shows that in the unconstrained case  $A/B$  keeps clear of  $L^{-2}$ , while in the constrained case it unmistakably reaches  $L^{-2}$ . Beyond this point  $\xi \sim L$ , so that  $A/B$  is no longer a good estimate of  $\xi^{-2}$ . This is exactly what we expect in a system with nonzero surface tension undergoing phase separation. We studied two other sizes,  $L = 8$  and  $L = 25$ , and in both cases  $A/B$  reaches  $L^{-2}$ , indicating phase separation. At higher temperatures, however, the correlation is enhanced by the constraint, but nonetheless  $A/B$  does not reach  $L^{-2}$  (Fig. 3, right). This is consistent with the idea that the surface tension decays at high temperature, thus preventing phase separation [22].

What we are doing here is very similar to switching from nonconserved to conserved dynamics in the Ising model,

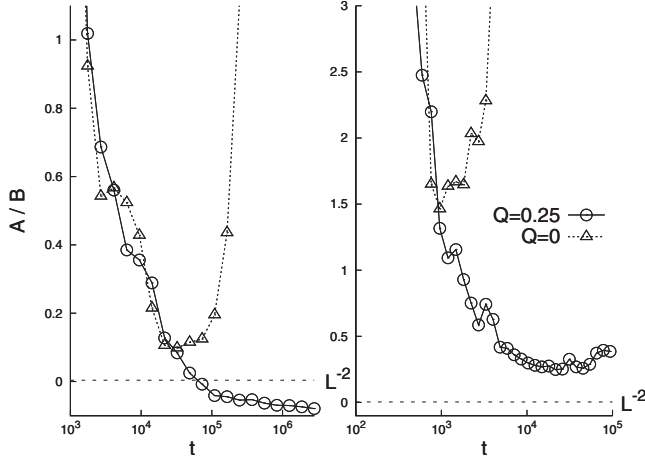


FIG. 3. Left: The estimator  $A/B$  [see Eq. (2)] vs time, at  $T = T_{MC}$  in the constrained (circles) and unconstrained (triangle) cases. Right: The same at  $T = 1.55T_{MC}$ .  $L = 16$ .

by constraining the order parameter (i.e., the magnetization) [23]. A very rich phenomenon that stands out in this context is coarsening. Coarsening contains information both on the surface tension (there would not be coarsening without it) and on the exponents relating the energy cost of the domains to their sizes. In systems with a conserved order parameter undergoing phase separation, the domain size  $\xi(t)$  grows as  $t^{1/3}$  and the dynamics proceeds by reducing the total amount of interfaces and, therefore, of energy. The interface energy per domain scales like  $\xi^\theta$ , where  $\theta$  is the surface tension exponent. The total number of domains is  $L^d/\xi^d$ , so that the total interface energy density is  $\Delta E(t) \sim 1/\xi(t)^{d-\theta} \sim 1/t^{(d-\theta)/3}$ . In the standard case (e.g., Ising)  $\theta = d - 1$ , so that  $\Delta E(t) \sim 1/t^{1/3}$  [20]. Figure 4 shows that something remarkably similar happens here. After the constraint kicks in,  $\Delta E(t)$  decays compatibly with an exponent  $1/3$ . Although fitting coarsening exponents is notoriously difficult, our data seem to be compatible with the “naive” exponent  $\theta = 2$  [22,24].

In general, phase separation is the landmark of first-order phase transitions and metastability. At the mean-field level, one can define a thermodynamic potential as a function of the order parameter that, below some spinodal point, exhibits a stable and a metastable minimum, corresponding to the two phases. In finite dimension Maxwell’s construction makes the potential convex, so that the potential is flat (zero second derivative) in a finite interval (Fig. 5, inset). Maxwell’s construction implies that when the order parameter is constrained to take a value in the nonconvex interval, phase separation occurs. We have clearly observed phase separation. Can we observe a thermodynamic potential with a flat region?

Our phase-separating order parameter is the overlap  $Q$ , so it is a potential  $W(Q)$  we are after. Besides,  $W(Q)$  must determine the observed probability distribution of  $Q$  through the relation  $P(Q) = \exp[-NW(Q)]\Theta(Q - \hat{Q})$  (the  $\Theta$  function enforces the constraint [25]). If we com-

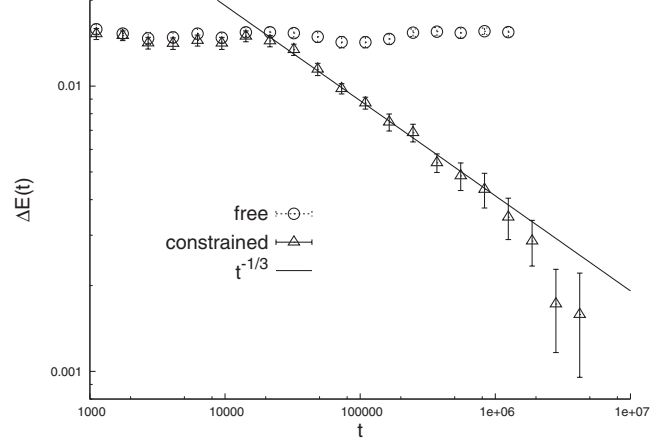


FIG. 4. Energy difference  $\Delta E(t) = E(t) - E_0$  vs  $t$  at  $T = T_{MC}$  with constrained dynamics,  $\hat{Q} = 0.25$ .  $E_0$  is a parameter of the fit  $E(t) = E_0 + \gamma t^{-1/3}$ . The line is  $1/t^{1/3}$ , corresponding to the surface tension exponent  $\theta = 2$ .

pute the average linear fluctuation of  $Q$  and expand the exponential, we obtain

$$W'(\hat{Q}) \sim N^{-1}\langle Q - \hat{Q} \rangle^{-1}. \quad (3)$$

This quantity we can compute by measuring the (very small) average fluctuation of the overlap once the constraint has been hit (see [26] for a different definition of the potential). We report  $W'(\hat{Q})$  in Fig. 5. The second derivative is clearly nonzero at high  $T$ , whereas around the mode-coupling temperature a finite region with  $W''(\hat{Q}) \sim 0$  develops. This is evidence of Maxwell’s construction, and it supports the link between phase separation and metastability. This result also explains another key point: If we constrain the overlap to a value large enough to fall in the nonflat region of the potential, then we observe no phase separation. Instead, the particles still overlapping when the constraint kicks in remain pinned forever, and no domain growth takes place.

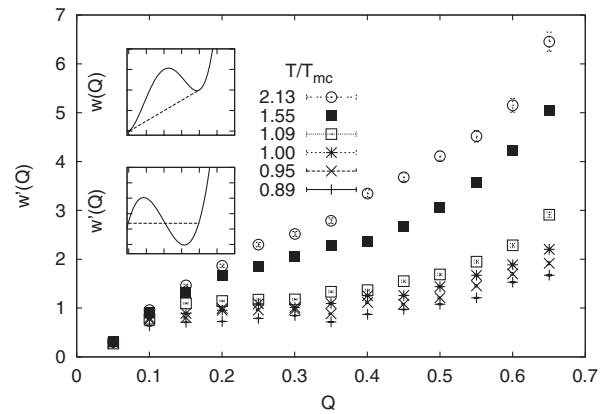


FIG. 5. The derivative  $W'(\hat{Q})$  of the thermodynamic potential at different temperatures, ranging from  $2.13T_{MC}$  to  $0.89T_{MC}$ . Inset: A cartoon of Maxwell’s construction for the potential and its derivative.

$W(Q)$  is a finite-dimensional variant of the two-replica potential introduced in mean-field theory [27,28]. This potential is the free energy cost to keep a configuration (the running one in the present work) at fixed overlap  $Q$  with a generic equilibrium configuration (the reference one). Below a dynamic transition (roughly, the mode-coupling temperature), the mean-field potential develops a metastable minimum at a finite value of  $Q$ . In this framework, relaxation at low temperatures can be interpreted as a barrier-crossing process, bringing the system from the metastable minimum (short times, finite  $Q$ ) to the stable minimum (long times, zero  $Q$ ) [29]. The constraint serves to keep the overlap within the nonconvex region of the potential and therefore force phase separation.

We have studied the dynamics of a glass-forming liquid with constrained global overlap. At low temperatures the system phase separates into regions of high and low overlap, as indicated by the dynamic correlation function and by the thermodynamic potential. This separation occurs in *real space*, and it is thus different from the separation in trajectory space recently reported [30]. On the contrary, there is no phase separation at high temperature, supporting the view that surface tension decreases at high  $T$ . The coexistence of regions belonging to different amorphous “states” (the high- or low-overlap patches) is reminiscent of the random first-order theory of thermodynamic relaxation [9]. In the dynamical case, the evolution of these regions is driven by a classic coarsening mechanism (stable with the constraint and ephemeral without it). In the thermodynamic case, the evolution of these regions is presumably driven by an entropic mechanism [9]. Our results show that surface tension and metastability stand as key links between the two frameworks.

We thank G. Biroli, J.-P. Bouchaud, L. Cugliandolo, S. Franz, W. Kob, and F. Zamponi for discussions and ECT\* and CINECA for computer time. T. S. G. was partly supported by ANPCyT, CONICET, and UNLP (Argentina). P. V. acknowledges support from MICINN through FIS2008-01323 and FIS2009-12648-C03-01.

\*Present address: CEA, Institut de Physique Théorique, Saclay, F-91191 Gif-sur-Yvette, France.

†Present address: SMC-INFM and Dipartimento di Fisica, Università di Roma “Sapienza,” piazzale Aldo Moro 5, 00185, Roma, Italy.

- [1] M. D. Ediger, *Annu. Rev. Phys. Chem.* **51**, 99 (2000).
- [2] C. Donati, S. C. Glotzer, and P. Poole, *Phys. Rev. Lett.* **82**, 5064 (1999).
- [3] C. Donati, S. Franz, G. Parisi, and S. C. Glotzer, *J. Non-Cryst. Solids* **307**, 215 (2002).
- [4] J.-P. Bouchaud and G. Biroli, *J. Chem. Phys.* **121**, 7347 (2004).
- [5] A. Montanari and G. Semerjian, *J. Stat. Phys.* **125**, 23 (2006).
- [6] A. Cavagna, T. S. Grigera, and P. Verrocchio, *Phys. Rev. Lett.* **98**, 187801 (2007).
- [7] G. Biroli, J.-P. Bouchaud, A. Cavagna, T. S. Grigera, and P. Verrocchio, *Nature Phys.* **4**, 771 (2008).
- [8] J. H. Gibbs and E. A. DiMarzio, *J. Chem. Phys.* **28**, 373 (1958).
- [9] T. Kirkpatrick, D. Thirumalai, and P. Wolynes, *Phys. Rev. A* **40**, 1045 (1989).
- [10] T. Castellani and A. Cavagna, *J. Stat. Mech.* (2005) P05012.
- [11] A. Montanari and S. Franz, *J. Phys. A* **40**, F251 (2007).
- [12] We simulate the 3D soft-sphere binary mixture [31] with parameters as in Ref. [7]. Simulations were done with a Metropolis Monte Carlo calculation with particle swaps [32]. The mode-coupling temperature for this system is  $T_{MC} = 0.226$  [33]. Our largest system has  $N = 16\,384$  particles in a box of length  $L = 25.4$ .
- [13] The side  $\ell$  of the cells is such that the probability of finding more than one particle in a single box is negligible.
- [14] S. Caracciolo, R. Edwards, A. Pelissetto, and A. Sokal, *Nucl. Phys.* **B403**, 475 (1993).
- [15] The so-called *second-moment* correlation length is obtained by computing  $A$  and  $B$  by using only the first two points [14]. However, we find that a linear fit to a few small- $k$  points gives equivalent results while lowering statistical errors.
- [16] N. Lacevic, F. W. Starr, T. B. Schroder, and S. C. Glotzer, *J. Chem. Phys.* **119**, 7372 (2003).
- [17] C. Toninelli, M. Wyart, L. Berthier, G. Biroli, and J. Bouchaud, *Phys. Rev. E* **71**, 041505 (2005).
- [18] Actually,  $Q = \ell^3 = 0.062\,876$  for uncorrelated configurations, while  $Q = 1$  for identical configurations.
- [19] To enforce the constraint the probability to accept a move is  $p = \min\{1, \exp^{-\Delta E/T}\}$  for  $Q' \geq \hat{Q}$  and  $p = 0$  for  $Q' < \hat{Q}$ , where  $Q'$  is the proposed value of the overlap.
- [20] A. Bray, *Adv. Phys.* **43**, 357 (1994).
- [21] Because of the constraint, the space integral of the correlation function is zero; hence, the single point  $S^{-1}(0, t) = [\int d\mathbf{r} G(\mathbf{r}, t)]^{-1}$  must be excluded from the analysis. This also implies that the dynamical susceptibility  $\chi(t) = S(0, t) = V[\langle Q^2(t) \rangle - \langle Q(t) \rangle^2]$  is trivially zero.
- [22] C. Cammarota, A. Cavagna, G. Gradenigo, T. S. Grigera, and P. Verrocchio, *J. Stat. Mech.* (2009) L12002.
- [23] A closer match is the Ising model in a *negative* magnetic field with constrained *positive* magnetization.
- [24] C. Cammarota, A. Cavagna, G. Gradenigo, T. S. Grigera, and P. Verrocchio, *J. Chem. Phys.* **131**, 194901 (2009).
- [25] G. Parisi, arXiv:0911.2265v1.
- [26] L. Fernandez, V. Martin-Mayor, and D. Yllanes, *Nucl. Phys.* **B807**, 424 (2009).
- [27] S. Franz and G. Parisi, *J. Phys. I (France)* **5**, 1401 (1995).
- [28] S. Franz and G. Parisi, *Physica (Amsterdam)* **261A**, 317 (1998).
- [29] S. Franz, *J. Stat. Mech.* (2005) P04001.
- [30] L. O. Hedges, R. L. Jack, J. P. Garraham, and D. Chandler, *Science* **323**, 1309 (2009).
- [31] B. Bernu, J. P. Hansen, Y. Hiwatari, and G. Pastore, *Phys. Rev. A* **36**, 4891 (1987).
- [32] T. S. Grigera and G. Parisi, *Phys. Rev. E* **63**, 045102(R) (2001).
- [33] J.-N. Roux, J.-L. Barrat, and J.-P. Hansen, *J. Phys. Condens. Matter* **1**, 7171 (1989).